Information-Seeking in Localization and Mission Planning of Multi-Agent Systems

Kyriakos Lite and Bernhard Rinner
Institute of Networked and Embedded Systems
University of Klagenfurt, Austria
Email: kyriakos.lite@aau.at, bernhard.rinner@aau.at

***Abstract*—Real-time and accurate position estimation is critical for various multi-robot applications and serves as a prerequisite for location-based multi-sensor data analysis. However, it is often impeded by energy, sensing, and processing limitations. In this work, we study the problem of information-seeking in localization and navigation in multi-agent systems, which aims to navigate mobile agents while reducing position errors. We formalize information-seeking as reducing spatial uncertainty and introduce an efficient motion controller based on artificial potential fields superimposing attractive, repulsive, and information-seeking forces. We evaluate the effect of information-seeking on localization and mission planning in a simulation study with non-collaborative and collaborative localization approaches.**

***Index Terms*—Multi-robot system; Cramér–Rao bound (CRB); Fisher information; spatial uncertainty; artificial potential fields**

I. Introduction

Position information is essential for many robotic systems since it strongly influences the robot's performance during task and mission execution. The availability of accurate position information is highly relevant in multi-robot systems where mission planning strongly depends on the position of the individual robots (e.g., [1]–[3]). It is also an important prerequisite for capturing, processing, and distributing multi-sensor data as its analysis often depends on location. Examples for location-based multi-media capturing, processing and distribution in multi-robot systems include automated multi-view drone cinematography [4], adaptive-video streaming in search-and-rescue applications [5], and networking and multi-media data distribution [6]. Satellite-based positioning systems such as GPS have been widely applied, but face known limitations concerning availability in indoor environments, accuracy, and resource requirements.

Network localization and navigation (NLN) [7] addresses this challenge of ubiquitous positioning in GPS-denied environments. According to NLN, a mobile node is able to infer its position by performing pairwise measurements with anchor nodes and other mobile nodes (i.e., spatial cooperation), and temporal filtering based on state-evolution models (i.e., spatio-temporal cooperation). Cooperation among mobile nodes improves the accuracy and the reliability of the position estimates [8] while eluding the necessity for intensive resources.

Considering navigation, there has been a considerable amount of research in control of multi-agent systems [9].

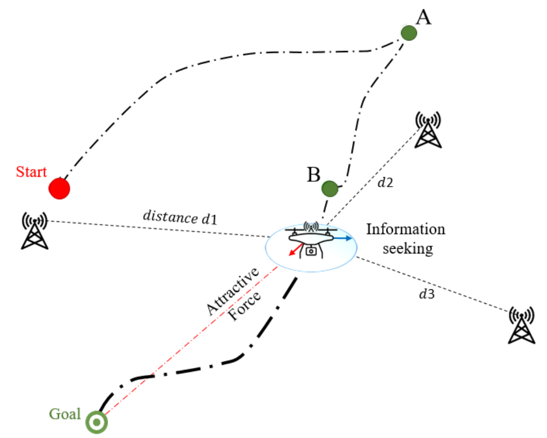

Fig. 1: Information-seeking localization and navigation with three anchors and one agent. The agent moves via waypoints A and B towards the goal in such a way that it reduces the uncertainty about its position.

Examples of such works focus on achieving mission objectives (e.g., goal approaching) while the agents maintain specific formations and avoid collisions with bio-inspired techniques such as flocking. The majority of these works consider the agents' locations to be known or augment them with noise to probe the robustness of the controller. There are only a few works that consider improving localization accuracy. For instance, Kim et al. [10] indirectly improve localization by optimizing the rigidity of a multi-agent system, while Meyer et al. [11] optimize the locations of the mobile agents by applying information-seeking in order to improve their own localization and the tracking of a target. Zhang et al. [12] focus on optimizing the positions of a swarm as a whole that uses Ultra-Wide band ranging technology to augment position information.

In this work, we consider systems that are able to perform RF-based range measurements via received signal strength [13] and formalize a lightweight controller that is aware of localization uncertainty. Our approach allows mobile nodes to accomplish their primary tasks (e.g., goal approaching and collision avoidance) while allowing them to navigate in a way that reduces the localization estimation error as illustrated in Fig. 1. In particular, we formalize the *information-seeking artificial potential fields* (IS-APF), by introducing the information-seeking force to the scheme. We show analytically how to derive the forces and conduct extensive simulations commenting on the emerged behaviors of the mobile agents.

II. Problem Formulation

In general, robotic systems operate in three dimensions (3-D) but for the sake of simplicity we consider a wireless localization network that resides in a two-dimensional (2-D) space. The network is composed of two types of nodes: N_a mobile agent nodes that require localization throughout their mission and N_b anchor nodes that have perfect knowledge of their position. Thus, the total number of nodes is $N = (N_a + N_b)$. Furthermore, we denote the position of node k by $p_k \in \mathbb{R}^2$ and the global location vector as $X = [p_1^T, p_2^T, \ldots, p_{Na}^T, p_{Na+1}^T, p_{Na+2}^T, \ldots, p_{Na+Nb}^T]$.

A. Localization

For every node i, $N-1$ received signal strength measurements to all other nodes j are available

$$\hat{P}_{i,j} = P_0 + 10n_p \cdot log(\frac{d_{i,j}}{d_0}) + n_{i,j} \tag{1}$$

where P_0 is the received power at a reference distance d_0. The parameter n_p = [2,…,4] is the pathloss exponent, $d_{i,j}$ is the Euclidean distance between nodes i and j, and $n_{i,j}$ represents additive white Gaussian noise with $\mu_{dB} = 0$ and σ_{dB}^2. We assume reciprocal signal strength measurements, i.e., $P_{i,j} = P_{j,i}$. We can convert the received signal strengths to distances by rearranging Equ. 1

$$\hat{d}_{i,j} = 10^{\frac{(P_0 - \hat{P}_{i,j})}{10n_p}}. \tag{2}$$

Furthermore, we define a connectivity vector $H_k(j)$ for every agent k with $j \in \{1, \ldots, N\}$ where $H_k(j) = 1$ if $\hat{d}_{k,j} < sens\_range$ else $H_k(j) = 0$.

The positions of the agents are estimated at each time step with a weighted least squares (WLS) estimator [14]

$$\begin{aligned}\hat{p} = \arg\min_p \sum_{k=1}^{N_a} \Bigg\{ & \sum_{i=1}^{N_a} H_k(i) \frac{1}{w_{ki}} (\hat{d}_{ki} - \|p_k - p_i\|)^2 \\ & + \sum_{j=N_a+1}^{N} H_k(j) \frac{1}{w_{kj}} (\hat{d}_{kj} - \|p_k - p_j\|)^2 \Bigg\}\end{aligned} \tag{3}$$

where w_{ki} and w_{kj} are weights defined as $\sqrt{(\sigma_{pos}^2 + \sigma_{dist}^2)}$ with σ_{pos} the position estimate variance and σ_{dist} the distance measurement variance, used to reflect the reliability of a measurement. Naturally, the position variance σ_{pos}^2 for the anchors is zero.

B. Dynamic System Formulation

The state of a generic node at time step t is its two-dimensional position (i.e., $p_k^{(t)} = [x_k^{(t)}, y_k^{(t)}]^T$). While the positions of the anchor nodes are known and fixed, the positions of the mobile agents are to be estimated and controlled. The agents move in a step-wise fashion according to the following movement model

$$p_k^{(t+1)} = p_k^{(t)} + u_k^{(t)} + \nu_k^{(t)} \tag{4}$$

where u_k is the control command and $\nu_k \sim N(0, \sigma_{tr}^2)$ the transition noise at time step t. The control command is derived as the superposition of the attractive, repulsive, and information-seeking forces

$$u_k^{(t)} = \mu(f_a^{(t)}(k) + f_r^{(t)}(k) + f_{is}^{(t)}(k)) \tag{5}$$

with μ as step size. We perform the state transition in single time steps using global force vectors $f_a, f_r, f_{is} \in \mathbb{R}^{2\times N_a}$ for all agents. In the following section, we show how to calculate the forces for every agent (cp. Fig. 2) which are then superimposed to form the global force vectors.

III. Multi-agent System Controller Formulation

A. Artificial Potential Fields

Artificial potential fields (APF) [15] is a well-known online path planning method where the environment is modelled by attractive and repulsive potentials and the robot moves towards the goal following the superposition of the two potential fields.

The attractive potential of agent k is a function of the agents' position p_k and its respective goal location p_{gk} and can be expressed as

$$U_a(k) = z_a \|p_{gk} - p_k\| \tag{6}$$

where z_a is a scaling factor. We assume that the agent has reached a goal location if $\|p_{gk} - p_k\| <= goal_{thres}$. The attractive force $f_a(k)$ is the negative gradient of the attractive potential

$$f_a(k) = -\nabla U_a(k) = z_a \frac{p_{gk} - p_k}{\|p_{gk} - p_k\|}. \tag{7}$$

The repulsive potential is a function of the agents' position and obstacles or other agents that need to be avoided. The potential can be expressed as

$$U_{ri}(k) = \begin{cases} \frac{z_r}{2}(\frac{1}{d_{ki}} - \frac{1}{\eta_{thres}})^2, & d_{ki} \le \eta_{thres} \\ 0, & d_{ki} > \eta_{thres} \end{cases} \tag{8}$$

where z_r is a scaling factor, η_{thres} is the influence range of the repulsive potential and d_{ki} is the Euclidean distance between agent k and agents (or obstacles) i with $i \in \{1, \ldots, N\}$ and $k \neq i$.

Similarly, the repulsive force f_r is defined as the negative gradient of the repulsive potential

$$f_{ri}(k) = -\nabla U_{ri}(k) = \begin{cases} \frac{z_r}{d_{ki}^2}(\frac{1}{d_{ki}} - \frac{1}{\eta_{thres}})\nabla d_{ki}, & d_{ki} \le \eta_{thres} \\ 0, & d_{ki} > \eta_{thres}. \end{cases} \tag{9}$$

When an agent is in the influence realm of one or more obstacles the total repulsive potential f_{Tr} of agent k is equal to:

$$f_{Tr}(k) = \sum_{i=1}^{N} f_{ri}(k) \tag{10}$$

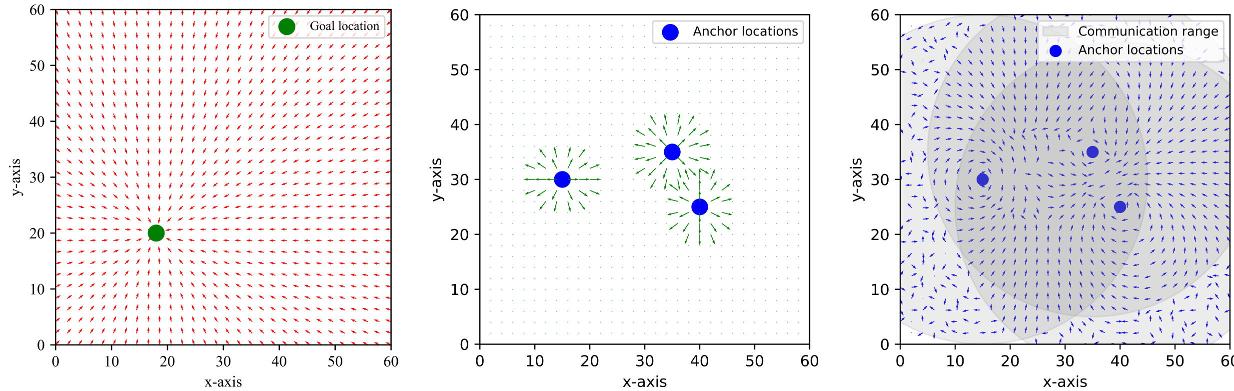

Fig. 2: The derived forces for our example scenario: (left) attractive force field in red, (center) repulsive force field in green, and (right) information-seeking force field in blue. Note that the force fields have been normalized for better readability.

B. Information Seeking

To account for localizability in the controller, we employ the mathematical tools of Fisher information (FI) theory and the Cramér–Rao bound (CRB). The CRB represents a theoretical limit of the best possible localization variance of any unbiased estimator with the following relation

$$\mathbb{E}[|p-\hat{p}|]^2 \geq CRB = trace(F_p^{-1}) \tag{11}$$

where F_p is the Fisher information matrix [8].

The aim of information seeking is to derive a force field that can direct an agent towards locations with minimal CRB. We follow a gradient approach to compute such field

$$\nabla CRB = \frac{\partial trace(F_p^{-1})}{\partial p}. \tag{12}$$

As noted in e.g., [16], (i) the derivative of a trace function of matrix A is the trace of the derivative

$$\frac{\partial trace(A)}{\partial p} = trace(\frac{\partial A}{\partial p}), \tag{13}$$

and (ii) the derivative of the inverse of A is equal to

$$\frac{\partial A^{-1}}{\partial p} = -A^{-1}\frac{\partial A}{\partial p}A^{-1}. \tag{14}$$

Thus, the derivative of the CRB can be computed as

$$\frac{\partial CRB}{\partial p} = -F_p^{-1}\frac{\partial F_p}{\partial p}F_p^{-1}. \tag{15}$$

By adopting [17] we compute the Fisher information matrix (FIM) and its partial derivatives with the following steps.

STEP 1: Calculate the partial derivatives of the Fisher information sub-matrices. Form six $N_A \times N_A$ matrices: dxF_{xx}, dxF_{xy}, dxF_{yy} for the x-axis and dyF_{xx}, dyF_{xy} and dyF_{yy} for the y-axis.

The sub-matrices for the x-axis can be computed as follows:

$$[dxF_{xx}]_{k,l} =$$

$$\begin{cases} \gamma \sum_{i \epsilon H_k} 2((x_k - x_i)d_{k,i}^2 - 4(x_k - x_i)^3)/d_{k,i}^6 & k = l \\ -\gamma H_k(l) 2((x_k - x_l)d_{k,l}^2 - 4(x_k - x_l)^3)/d_{k,l}^6 & k \neq l \end{cases}$$

$$[dxF_{xy}]_{k,l} =$$

$$\begin{cases} \gamma \sum_{i \epsilon H_k} ((y_k - y_i)(d_{k,i}^2 - 4(x_k - x_i)^2)/d_{k,i}^6 & k = l \\ -\gamma H_k(l)((y_k - y_l)(d_{k,l}^2 - 4(x_k - x_l)^2)/d_{k,l}^6 & k \neq l \end{cases}$$

$$[dxF_{yy}]_{k,l} =$$

$$\begin{cases} \gamma \sum_{i \epsilon H_k} -4(x_k - x_i)(y_k - y_i)^2/d_{k,i}^6 & k = l \\ \gamma H_k(l) 4(x_k - x_l)(y_k - y_l)^2/d_{k,l}^6 & k \neq l \end{cases} \tag{16}$$

We apply the same calculations for the second dimension.

Note that γ is a channel parameter and is equal to $((10n_p)/(\sigma_{dB} log10))^2$ and k, l are the indices of the matrix elements.

STEP 2: Merge the sub-matrices to form the partials of the FIM along the x and y axis. We create two $2N_A \times 2N_A$ matrices which hold the derivative of the FIM along the x and y axis, respectively:

$$F_{dx} = \begin{bmatrix} dxF_{xx} & dxF_{xy} \\ dxF_{xy}^T & dxF_{yy} \end{bmatrix}, F_{dy} = \begin{bmatrix} dyF_{xx} & dyF_{xy} \\ dyF_{xy}^T & dyF_{yy} \end{bmatrix} \tag{17}$$

STEP 3: Calculate the gradient components for every agent. We calculate the derivatives of the CRB along the x and y axis as:

$$\begin{aligned} CRB_{dx} &= -F_p^{-1}F_{dx}F_p^{-1} \\ CRB_{dy} &= -F_p^{-1}F_{dy}F_p^{-1} \end{aligned} \tag{18}$$

Then, the gradient components for an arbitrary agent k are given by:

$$c_{is}(k) = \begin{bmatrix} CRB_{dx}(k,k) + CRB_{dx}(k+N_a, k+N_a) \\ CRB_{dy}(k,k) + CRB_{dy}(k+N_a, k+N_a) \end{bmatrix} \tag{19}$$

Finally, the information seeking force for agent k is given as

$$f_{is}(k) = -z_{is}\frac{c_{is}(k)}{\|c_{is}(k)\|} \tag{20}$$

where z_{is}, is a weighting scalar.

IV. Simulation Study

We developed a simulation environment in Python to evaluate our IS-APF-based controller. A simulation is initialized with the desired locations of the agents, their respective goal locations, and the locations of the anchors. Table I summarizes the key simulation parameters. The controller is evaluated at every location and the agents move in a step-wise fashion. We perform hundred location estimations at every location to compute the root mean square error (RMSE). The simulation is terminated when the agents have completed successfully their missions or a mission duration threshold is reached.

We evaluate two simulation scenarios. In the *non-collaborative* scenario, a mobile agent has to navigate in an environment by performing range measurements with three anchor nodes in order to localize itself. In particular, the agent's mission is to pass through a number of predefined way-points, and connectivity to the anchor nodes is given throughout the mission. In the *collaborative* scenario two mobile agents have to complete their individual mission (i.e., sequence of way-points) in an environment with five anchors. Due to the settings of the mission, the agents intermittently lose connectivity to some anchor nodes as well as to each other.

We study the influence of information-seeking on the spatial uncertainty of the agents while navigating through the environment. We compare both scenarios under ideal conditions (i.e., perfect transition and localization) and under more realistic conditions (i.e., imperfect transition and estimated positions).

Table I: Simulation settings.

Ranging	IS-APF
$P_0 = -36\,dB$	$z_a = 1$
$d_0 = 1\,m$	$z_r = 50$
$n_p = 2.3$	$z_{is} = [0.0, ..., 0.9]$
$\sigma_{db} = 0.5\,dB$	$\eta_{thres} = 4\,m$
$sens\_range = 30\,m$	$goal_{thres} = 0.10\,m$
-	$\sigma_{tr} = 10^{-3}\,m$
-	$\mu = 0.2$

A. Discussion

1) Non-collaborative scenario: Fig. 3 (a) shows the effect of information-seeking on the mission paths by our IS-APF controller using the agent's true position data. The blue line represents the path of a traditional APF controller (without information-seeking) whereas the other colors represent paths with different weights for information-seeking. The IS-APF controller generates paths that reach the navigation way-points with lower spatial uncertainty (i.e., reducing the CRB). In some more detail, information-seeking reduces the effect of adverse geometry for localization along the first segment (avoid moving closely along the line between the two upper anchors). For the other two segments, information-seeking aims to move towards localization sweet spots (positions with low CRB within the anchor triangle). The paths deviate stronger from the traditional case with increasing information-seeking weights. Consequently, path length and mission duration increase as well (cp. Fig. 4).

Fig. 3 (c) depicts the lower bound on the RMS of localization error ($\sqrt{tr(CRB)/N_a}$) while the agent moves along the path. We can identify way-point A as the maximum value in these graphs and way-point B as the local maximum after the global minimum. The reduction of the spatial uncertainty can be clearly seen in the first segment and in the second segment where the global minimum decreases with increasing weight. This is also indicated with the red dotted line.

Fig. 3 (b) shows the effect of information-seeking on the mission paths by our IS-APF controller using the agent's estimated position data. We can observe a similar trend of the paths, but the executed trajectories include quite some fluctuations imposed by the noisy position estimation. Furthermore, there are some oscillations when agents approach the way-points. These oscillations result from inaccurate distance measurements, transition noise and the conical attractive force which can cause the agent to overshoot the target. Fluctuations and oscillations significantly increase the path length and mission duration (cp. Fig. 4). As depicted in Fig. 3 (d), strong fluctuations can also be observed in the estimated RMS error which is given as $\sqrt{\mathbb{E}\{\|p-\hat{p}\|^2\}/N_a}$ for each step. In comparison with Fig. 3 (c), the global minima do not significantly decrease with increasing weights.

2) Collaborative scenario: In the collaborative scenario, the information-seeking force field becomes dynamic as it is influenced by mobile agents. Fig. 5 depicts the CRB values for this scenario. However, no clear CRB reduction with increasing z_{is} is observable as in the non-collaborative scenario. Two elongated periods with low CRB values occur for $z_{is} = 0.4$ and 0.7. This is visible in Fig. 6 (b) were the trajectory of the agent in blue persists above the middle anchor throughout the mission.

As shown in Fig. 6, the agents perform their individual missions avoiding collision with each other and the center anchor node. For $z_{is} = 0.4$, the trajectories become curvier due to the information-seeking force pulling the agents towards locations of lower CRB. Additionally, in this particular collaborative scenario, the mission time does not necessarily increase with z_{is} (see Fig. 5) as was observed in the non-collaborative scenario. Due to the information-seeking force completely different paths can be chosen. If the IS-APF controller uses position estimates (see Fig. 6 (c,d)) the agents maintain the nominal path in general, but oscillations appear when agents approach way-points. In extreme cases, oscillations may continue for long periods, and the agent is not able to complete its mission.

V. Conclusions and Future Work

In this work we extended the APF controller to account for reducing the spatial uncertainty by introducing an information-seeking potential. We analytically derived the different force fields and conducted a simulation study on a non-collaborative

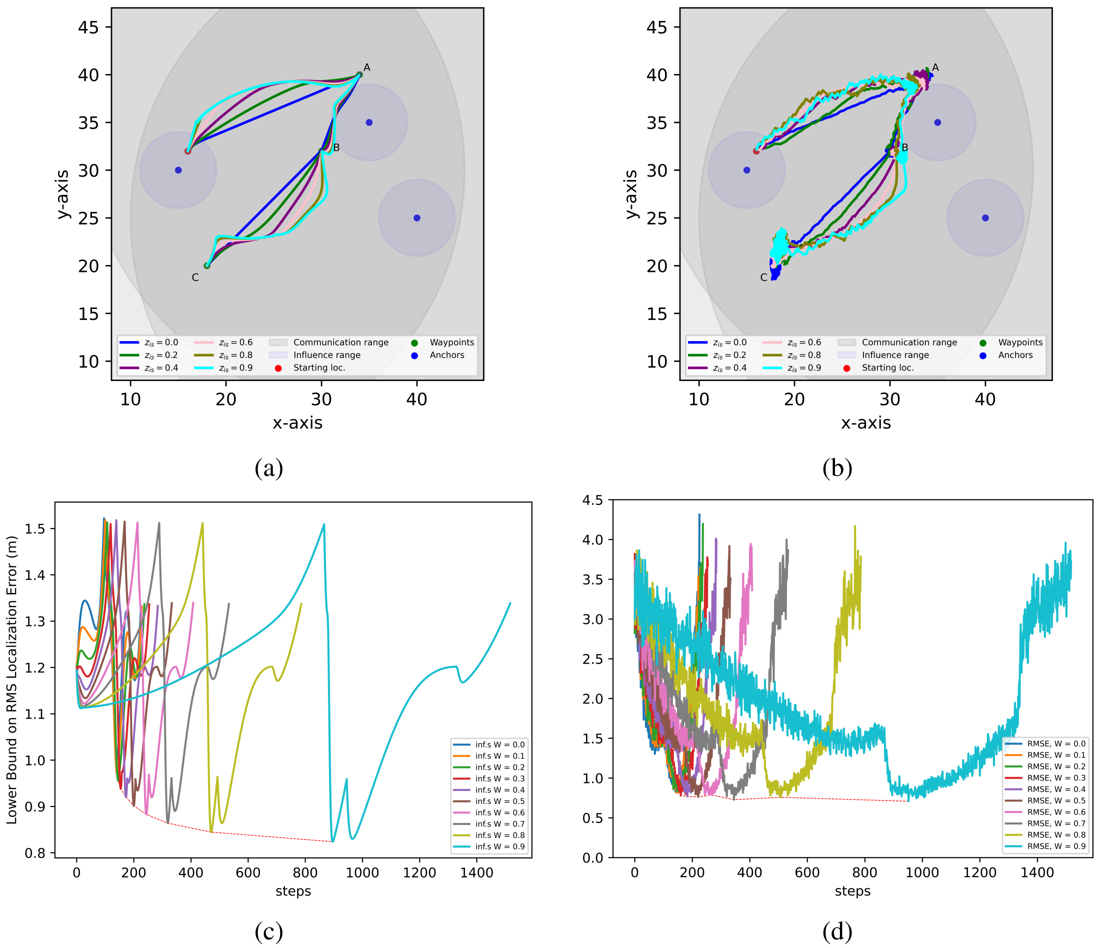

Fig. 3: Comparison of the computed paths through way-points A, B, and C with different weights for the information-seeking force field (top row) and the position uncertainty of the agent expressed by the CRB (bottom row). Plot (a) shows the paths executed by our IS-APF controller using the agent's true position, whereas plot (b) shows paths derived from estimated agent's positions. Graph (c) depicts the CRB along the mission executed using the true positions and graph (d) depicts the estimated RMS error of the agent's position.

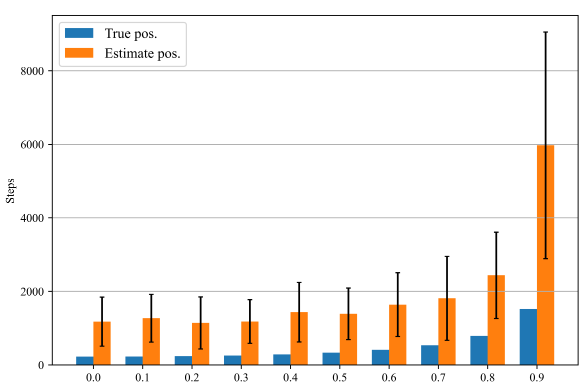

Fig. 4: Simulation steps required to complete the mission for the IS-APF controller using the true agent's positions (blue) and the estimated positions (orange) with different weights z_{is}. Whiskers represent the standard deviation of 100 simulation runs.

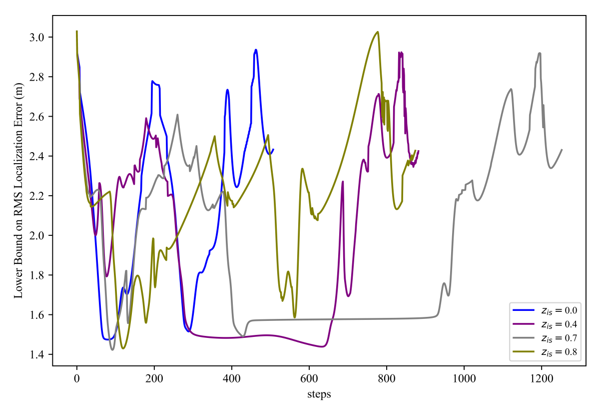

Fig. 5: CRB plot of the collaborative scenario. Elongated periods of low CRB values are achieved for $z_{is} = 0.4$ and 0.7. Note that the mission duration is shorter for $z_{is} = 0.8$ than for $z_{is} = 0.8$.

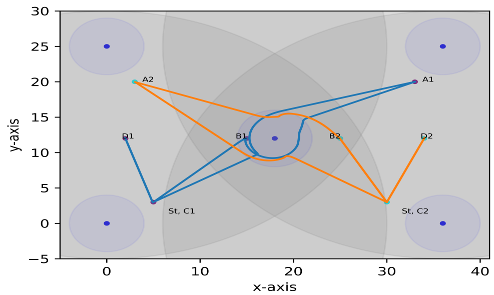

(a) $z_{is} = 0.0$.

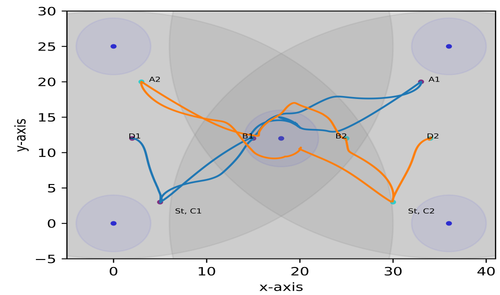

(b) $z_{is} = 0.4$.

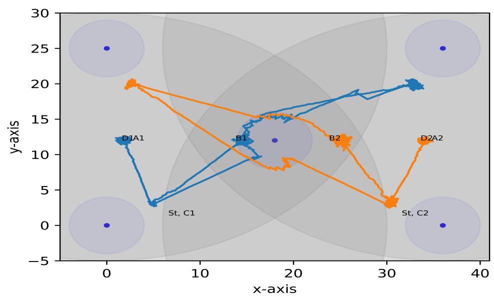

(c) $z_{is} = 0.0$.

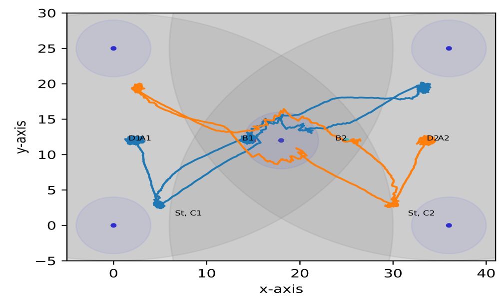

(d) $z_{is} = 0.4$.

Fig. 6: Comparison of the of the executed paths in the collaborative scenario. The top row shows the paths based on true position data, whereas the bottom row shows paths based on estimated position. The left column shows paths generated from a traditional APF controller, whereas the right column shows the graphs with IS-APF controller with $z_{is} = 0.4$.

and collaborative localization scenario. We showed that IS-APF, can be used by agents to safely navigate the environment while minimizing spatial uncertainty.

As future work we plan to further improve the IS-APF controller by dynamically adapting the weights to avoid the antagonizing effect of attractive and information-seeking forces and by introducing a combinatorial attractive potential [15] with smoother force profiles near way-points. Finally, we want to deploy information-seeking in multi-robots and support location-based multi-media analysis.

References

[1] Yara Rizk, Mariette Awad, and Edward W Tunstel. Cooperative heterogeneous multi-robot systems: A survey. *ACM Computing Surveys (CSUR)*, 52(2):1–31, 2019.

[2] Bernhard Rinner, Christian Bettstetter, Hermann Hellwagner, and Stephan Weiss. Multidrone systems: More than the sum of the parts. *IEEE Computer*, 54(5):34–43, 2021.

[3] Petra Mazdin and Bernhard Rinner. Distributed and communication-aware coalition formation and task assignment in multi-robot systems. *IEEE Access*, 9:35088–35100, 2021.

[4] Tobias Nägeli, Lukas Meier, Alexander Domahidi, Javier Alonso-Mora, and Otmar Hilliges. Real-time planning for automated multi-view drone cinematography. *ACM Transactions on Graphics*, 36(4), 2017.

[5] Jürgen Scherer, Saeed Yahyanejad, Samira Hayat, Evsen Yanmaz, Torsten Andre, Asif Khan, Vladimir Vukadinovic, Christian Bettstetter, Hermann Hellwagner, and Bernhard Rinner. An autonomous multi-uav system for search and rescue. In *Proceedings of the 13th International Conference on Mobile Systems, Applications, and Services*, Florence, Italy, 2015. ACM.

[6] Samira Hayat, Evsen Yanmaz, and Raheeb Muzaffar. Survey on unmanned aerial vehicle networks for civil applications: A communications viewpoint. *IEEE Communications Surveys and Tutorials*, 16(4):2624–2661, 2016.

[7] Moe Z. Win, Andrea Conti, Santiago Mazuelas, Yuan Shen, Wesley M. Gifford, Davide Dardari, and Marco Chiani. Network localization and navigation via cooperation. *IEEE Communications Magazine*, 49(5):56–62, 2011.

[8] Yuan Shen, Henk Wymeersch, and Moe Z. Win. Fundamental limits of wideband localization— part ii: Cooperative networks. *IEEE Transactions on Information Theory*, 56(10):4981–5000, 2010.

[9] Kwang-Kyo Oh, Myoung-Chul Park, and Hyo-Sung Ahn. A survey of multi-agent formation control. *Automatica*, 53:424–440, 2015.

[10] Yanghyun Kim, Guangwei Zhu, and Jianghai Hu. Optimizing formation rigidity under connectivity constraints. In *49th IEEE Conference on Decision and Control (CDC)*, pages 6590–6595, 2010.

[11] Florian Meyer, Henk Wymeersch, Markus Fröhle, and Franz Hlawatsch. Distributed estimation with information-seeking control in agent networks. *IEEE Journal on Selected Areas in Communications*, 33(11):2439–2456, 2015.

[12] Siwei Zhang, Robert Pöhlmann, Thomas Wiedemann, Armin Dammann, Henk Wymeersch, and Peter Adam Hoeher. Self-aware swarm navigation in autonomous exploration missions. *Proceedings of the IEEE*, 108(7):1168–1195, 2020.

[13] Xinrong Li. Collaborative localization with received-signal strength in wireless sensor networks. *IEEE Transactions on Vehicular Technology*, 56(6):3807–3817, 2007.

[14] R. Michael Buehrer, Henk Wymeersch, and Reza Monir Vaghefi. Collaborative sensor network localization: Algorithms and practical issues. *Proceedings of the IEEE*, 106(6):1089–1114, 2018.

[15] B. Siciliano, L. Sciavicco, L. Villani, and G. Oriolo. *Robotics: Modelling, Planning and Control*. Advanced Textbooks in Control and Signal Processing. Springer London, 2010.

[16] Jan R. Magnus and Heinz Neudecker. *Matrix Differential Calculus with Applications in Statistics and Econometrics*. John Wiley, second edition, 1999.

[17] N. Patwari, J.N. Ash, S. Kyperountas, A.O. Hero, R.L. Moses, and N.S. Correal. Locating the nodes: cooperative localization in wireless sensor networks. *IEEE Signal Processing Magazine*, 22(4):54–69, 2005.